Gamma Ray Spectroscopy

Nicholas Harris, David Pendergrass, Jeffrey Roe
Lab 15 Report, Group 5
5/10/2010

Contents

1 Abstract

Nuclear decay is a property exhibited by many elements and is a widely studied topic in modern physics. When the nucleus of an unstable atom transitions to a lower energy state, the decay manifests itself through the emission of either particles or photons. If the decay emits positrons, it is possible that these positrons will annihilate with their anti-particle counterpart (electrons) in the surrounding atoms, an interaction which will also emit photons. If the photons emitted in the nuclear decay process are within an energy range 100 keV to 10 MeV, they are known as "gamma rays". A tool known as a "scintillation counter" allows the effective and accurate detection of the gamma ray energy spectra emitted in these interactions.

There are several interactions which can take place between the gamma rays and the atoms in the detection apparatus that must be accounted for when analyzing a spectrum obtained through scintillation. Being aware of these allows for the theoretical determination of the spectrum properties that should be exhibited by a decaying nucleus. By comparing various elements gamma ray spectra obtained through scintillation to these theoretical results, it is possible to verify the existing theory, as well as make predictions based on the assumption that the theory is correct. Namely, the constitute elements of an unknown source can be determined. A prediction of the electron rest mass can also be found.

The mechanisms that contribute to the various properties of a decaying source's gamma ray spectrum also become apparent when a material is placed between a decaying source and the detector (a "shield"). Most specifically, these mechanisms are evident in the reduction of the number of photons able to reach the detector from the source material, a process known as "gamma ray attenuation". The effectiveness of a specific material to attenuate incident gamma rays can be quantified by a material property known as the "density normalized mass attenuation coefficient". This coefficient can be determined by analyzing the decrease in the number of photons of certain energy detected as the thickness of the shield is increased.

In this experiment, scintillation was used to analyze the spectra of various radioactive sources in order to experimentally verify existing decay theories, determine the composition ratio of an unknown source, predict the rest mass of the electron, as well as determine the density normalized mass attenuation coefficient of lead and copper at both a low and high gamma ray energy range.

2 Introduction

The term gamma ray refers to electromagnetic radiation (or "photons") in the energy range 100 keV to 10 MeV. When certain types of nuclei decay, the decay results in the output of unique gamma ray energies, corresponding to the nuclear de-excitations taking place. Aside from just the photons emitted from the decay itself, anti-protons that are produced during the nuclear decay can also collide with electrons in the atom to create two photons with energies 511 keV. A common tool used to detect gamma rays emitted by an unstable nucleus is a scintillation counter. By using scintillation counter to detect the energy of the incoming photons and recognizing the mechanisms involved in their creation and detection, atomic nuclei and their decay products can be studied.

2.1 Scintillation Counter

Radiation that is incident on certain materials produces a small flash of light. This light, when exposed to a semiconductor device known as a "photomultiplier", can be detected. The photomultiplier signal is proportional to the amount of light it receives, and because the materials used to produce the light emit photons in proportion to the radiation energy, the photomultiplier signal is therefore proportional to this incoming energy. This combination of a "scintillation" material in conjunction with a photomultiplier tube is known as a "scintillation" counter, and is an effective tool for obtaining and analyzing the spectra of gamma ray emissions due to nuclear decay. For this experiment, a "NaI(Tl)" scintillation counter was used. This type of detector uses a sodium iodide crystal, with a trace of thallium to achieve the scintillation of the incoming gamma rays.

2.2 The Photoelectric Effect

The primary mechanism responsible for the detection of the gamma rays in the scintillation detector is the photoelectric effect. This effect describes the absorption of the entire gamma ray energy by electrons in the detector crystal. When this occurs, the incident photon is completely annihilated, and the newly energized electron will have enough energy to escape the atoms in the crystal, thereby leading to a peak in the detected spectrum at the corresponding energy. This peak is referred to as the "full absorption peak" or "photopeak" and should be present in all nuclei emitting radiation in the gamma ray spectrum.

2.3 The Compton Effect

A second effect present in the spectrum of nuclear gamma rays when detected through scintillation is the Compton effect. This describes the inelastic collision of a nuclear ejected photon and an electron in the detector crystal. When it occurs, the photon both changes its direction and imparts some of its energy to the electron. The photon exits the detector crystal, due to this change in direction; however, the newly energized electron is left behind to be detected. This process can lead to "peaks" in gamma ray spectrum that span a wide range of energies, all of which are of lower than the full absorption peak, since only some of the original photon's energy is given to the electron. The energy of the electron detected is the difference in the energy of the original gamma ray and the scattered ray, which can be calculated upon determining the angle at which it is scattered:

$$E_{elec} = E_{\gamma}\left(1 - \frac{mc^2}{E_{\gamma}(1 - cos\theta) + mc^2}\right).$$

Here, E_{γ} is the original photon energy, mc^2 is the electron's rest mass, and θ is the angle of the scattered photon. From this formula, the maximum amount of energy that can be transferred to the electron through Compton scattering (known as the Compton edge") can be computed. It is given by the photons scattered back at 180 degrees and has the formula

$$E_{ce} = \frac{2E_\gamma{}^2}{mc^2 + 2E_\gamma}.$$

The Compton effect also accounts for the so-called "backscatter" peak in the detected photon spectrum. This peak is caused by photons that would have originally escaped the detection crystal being Compton scattered back into the detector by electrons in the material surrounding the detector. Only those photons "backscattered" at angles around 180 degrees will be detected, therefore leading to another peak in the gamma ray spectrum, theoretically given by

$$E_{bs} = \frac{2E_\gamma}{1 + 2E_\gamma/mc^2}.$$

2.4 Pair Production

A third mechanism that contributes peaks to the detected gamma ray spectrum is pair production. Pair production leads to additional peaks in the spectrum not due to photons produced in the nuclear decay itself. One way this can occur is through the creation of a positron as a bi-product of the nuclear decay. Since the positron is the anti-particle of the electron, those emitted in the nuclear decay often encounter electrons in the surrounding atoms of the source material, annihilating into two photons with energy 511 keV upon the collision. One of the two emitted photons will then be able to travel to the detector, where it will cause a peak in the gamma ray spectrum at 511 keV. Another way pair production can affect the photon peaks detected is by pairs being created inside the detector and quickly annihilating. If the nucleus releases gamma rays with energy higher than 1.022 MeV, these photons will be able to created electron-positron pairs inside the detector crystal. These newly created particles combine back together quickly, annihilating each other and releasing another photon with the same energy as the original that created the pair. These high energy gamma rays will then be detected through scintillation and lead to a peak of high energy in the gamma ray spectrum.

2.5 Rayleigh Scattering

Rayleigh scattering describes the elastic scattering of the photons in the detector. With elastic scattering, the energy of the scattered photons is the same as the original photons, so there is no new peak present corresponding to this mechanism. It does, however, change the direction of the incoming photon which can cause the photon to be redirected outside of the detection area. Therefore, the Rayleigh effect results in a reduction in the overall intensity of the primary absorption peak, not in any new peaks in the spectrum.

2.6 Gamma Ray Attenuation

When a material is placed between the detector and the gamma ray source, the processes described in the previous sections (2.2-2.5) that take place within this material (the "shield"),

affectively decreasing the number of incident gamma rays that make it to the scintillation counter to be detected. The effectiveness of a specific material for shielding gamma rays of certain energy is contained in a material property known as the "mass attenuation coefficient", denoted by μ. Each of the mechanisms described previously has its own specific contribution to the attenuation coefficient; however, it is typical that these different sources of attenuation are left undistinguished, giving an overall attenuation coefficient that is a composite of the four sources:

$$\mu = \mu_{pe} + \mu_{ray} + \mu_{comp} + \mu_{pp} .$$

Here μ_{pe}, μ_{ray}, μ_{comp}, μ_{pp}, are the contributions to the overall attenuation coefficient from the photoelectric effect, Rayleigh scattering, the Compton effect and pair production, respectively. Using this generalized coefficient, it is found that the change in the number of photons detected can be represented by the equation

$$\Delta N = N_0(\rho x)\left(\frac{\mu}{\rho}\right)$$

where ρ is the density of the material, x is the thickness of the shield, and μ/ρ is the "density normalized mass attenuation coefficient" which typically is found in units of g/cm^2. The solution of this equation is given by

$$N = N_0 e^{-(\rho x)(\mu/\rho)} .$$

If the natural logarithm of both sides of this equation is taken, this becomes

$$\ln N = \ln N_0 - \left(\frac{\mu}{\rho}\right)(\rho x) .$$

Therefore, a plot of the logarithm of the gamma ray peak intensity versus the shield material density multiplied by the shield thickness should yield a line whose slope is the negative of the density normalized mass attenuation coefficient.

3 Procedure

3.1 Low Energy Gamma Ray Detection

3.1.1 Calibration for Low Energy Decay

The UC-30 software was first calibrated for the detection of gamma rays in the range of 0 to 1 MeV. The software is equipped with an "auto-calibration" function that uses a ^{137}Cs source that is practical for these energies. The ^{137}Cs source was place on top of a lead brick and a cylindrical lead

shield was placed around it. The NaI(Tl) detector was then inserted into the cylindrical shield and the auto-calibration feature used to calibrate the software.

3.1.2 Low Energy Decay Detection

The sources known to emit low energy gamma rays were then inserted into the lead cylinder individually, and the software was used to obtain the gamma ray emission spectra for each of them. The sources known to emit lower energy photons were ^{137}Cs, ^{133}Ba, ^{109}Cd, ^{57}Co, and ^{54}Mn. Using these acquired spectra, the properties of the spectra and nuclear decay discussed previously could be analyzed. This also allowed for the determination of the electron rest mass (mc^2). Some of the sources (^{207}Bi and the unknown source), are known to emit gamma rays within both the low energy (<1 MeV) and the high energy (> 1 MeV) range. A spectrum for these elements was taken with the low energy calibration so that their properties in this range could be examined.

3.2 High Energy Gamma Ray Detection

3.2.1 Calibration for High Energy Decay

As discussed in (3.1.1), the auto-calibration feature is most useful for measuring photon energies below 1 MeV. Some of the sources being analyzed, however, exhibit emission spectra containing energies above this. Therefore, a manual, two-point calibration was done using the ^{22}Na source that allowed for the accurate measurement of gamma rays above 1 MeV. The ^{22}Na source was placed in the cylinder and the detector was placed on top of it. The previous calibration (from the ^{137}Cs source) was cleared from the software. The "base" spectrum was then obtained by the software, which showed the relative peaks in the spectra with no energy scale. Two of the peaks in this spectrum were then defined by taking the 511 keV and 1275 keV peaks as known quantities. This allowed the software to accurately determine the energy scale for the subsequent measurements.

3.2.2 High Energy Decay Detection

Similarly to the procedure with the lower energy sources, each of the sources known to emit high energy gamma rays was individual placed into the lead cylinder, the detector place on top of it, and a spectrum obtain with the software. The two sources examined were ^{22}Na and ^{60}Co. With these spectra, it was then possible to analyze the mechanism responsible for each of the peaks as well as determine a value for the electron rest mass (mc^2). High energy spectra were also obtained for two sources known to exhibit both low and high energy radiation peaks (^{207}Bi and the unknown source), allowing for the analysis of these nuclear decays at the higher energy range.

3.3 Density Normalized Mass Attenuation Coefficient

3.3.1 Low Energy Coefficient

For the determination of the density normalized mass attenuation coefficient of lead and copper at lower energies, the auto-calibration of the UC-30 software with ^{137}Cs was used as described in 3.1.1. For this portion of the procedure, the reduction of the 136 keV peak of ^{57}Co was analyzed as the thickness of the shield placed between the detector and the source was increased. First, a spectrum was taken for the source with no shield present and the number of counts obtained for the 122 and 136 keV peaks were noted. A lead sheet of 0.369 mm (whose thickness was measured with calipers) was then inserted in between the source and the detector and a spectrum was again taken. This was repeated for an increasing number of sheets until the number of 122 and 136 keV peak counts were at least a third of its original value with no shield. The lead was then removed and the same steps were repeated using a copper shield.

3.3.2 High Energy Coefficient

The procedure followed for determining the value of the higher energy gamma ray attenuation coefficient was similar to that as for its low energy counterpart (3.3.1). The calibration, however, was done using ^{22}Na source and the two point manual calibration function of the UC-30 software (3.2.1). For the analysis of high energy gamma ray attenuation, the ^{60}Co source was used and its 1173 and 1333 keV peaks were examined when attenuated with both lead and copper. Just as in the lower energy procedure, a spectrum was taken for the ^{60}Co source with no shield. Lead sheets were then measured and inserted between the source and the detector, using the UC-30 software to obtain a spectrum upon each insertion. This was done until the resulting spectrum showed an intensity reduction of three times that of the original 1173 and 1333 keV peaks with no shield. After this was achieved, the lead was removed from the setup and the same steps repeated with copper.

4 Results and Discussion

4.1 Known Sources

4.1.1 Theoretical Results

Using the theory given in the introduction section, the theoretical values of the backscatter and Compton edge peaks were calculated. These results can be seen in Table 1 of the appendix. These values were used in the following analysis to compare the theoretically determined peaks to those obtained in the experiment through scintillation. These results can be seen in Table 2 of the appendix.

4.1.2 Experimental Results

4.1.2a ^{133}Ba

There were three large photopeaks found for ^{133}Ba, as seen in Figure 1. The first, at 87 keV, has an associated Compton edge at 30 keV and backscatter peak at 68 keV. These values deviate from the expected values by 7.4%, 53.8%, and 10.6%, respectively. The large error associated with the Compton edge is due to the low energy value of the edge. The next, at 310 keV, has an associated Compton edge at 169 keV and backscatter peak at 124 keV. These values deviate from the expected values by 2.3%, 2.8%, and 10.5%, respectively. The last, at 370 keV, has an associated Compton edge at 207 and backscatter peak at 154 keV. These values deviate from the expected values by 3.6%, 10.2%, and 0.4%, respectively.

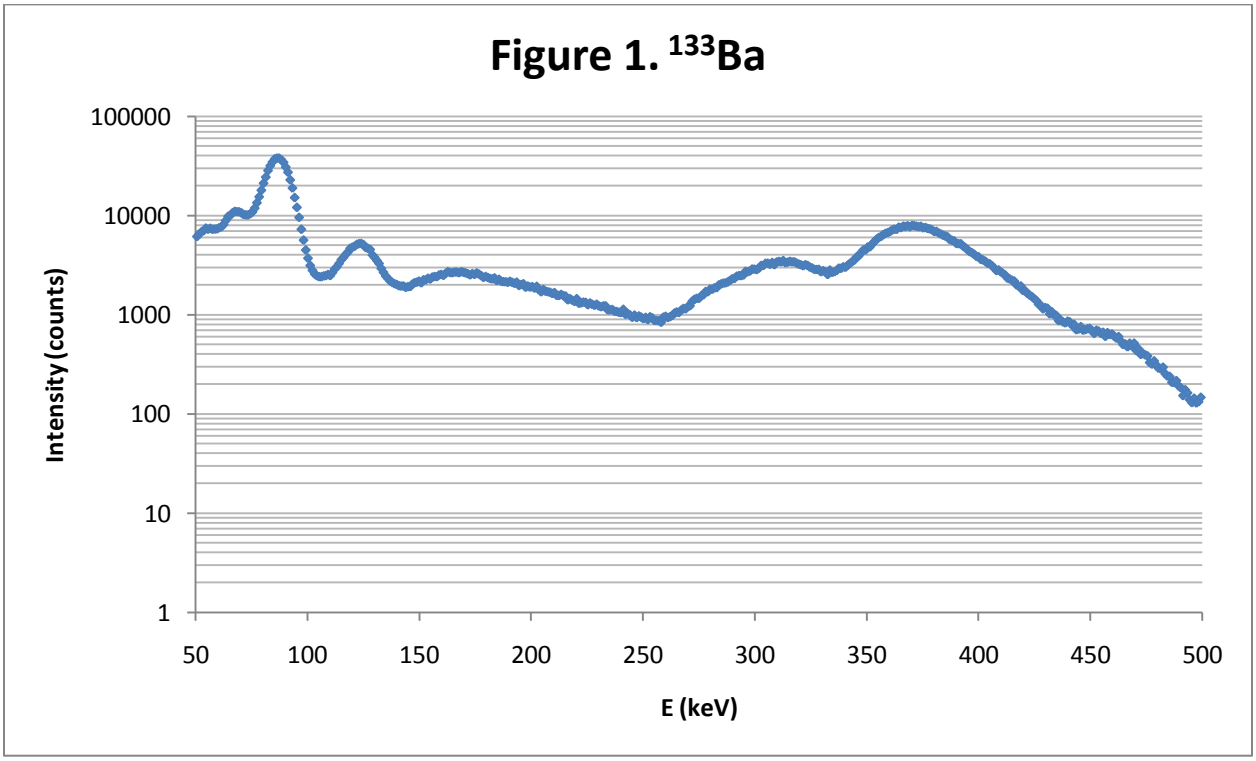

4.1.2b ^{109}Cd

There was one photopeak found for ^{109}Cd, as seen in Figure 2. The peak, at 93 keV, has an associated Compton edge at 21 keV and backscatter peak at 76 keV. These values deviate from the expected values by 5.7%, 6.9%, and 16.1%, respectively.

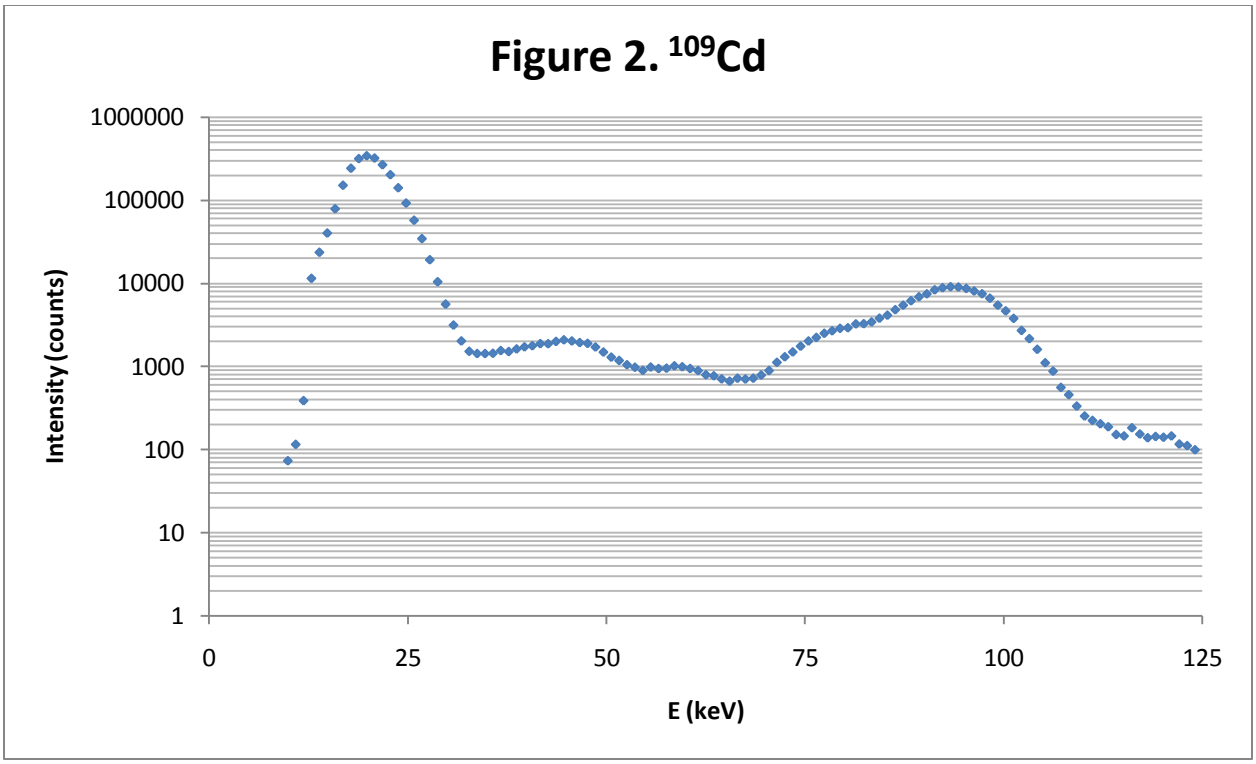

4.1.2c ^{137}Cs

There was one photopeak found for ^{137}Cs, as seen in Figure 3. The peak, at 663 keV, has an associated Compton edge at 454 keV and backscatter peak at 205 keV. These values deviate from the expected values by 0.2%, 5.0%, and 11.2%, respectively.

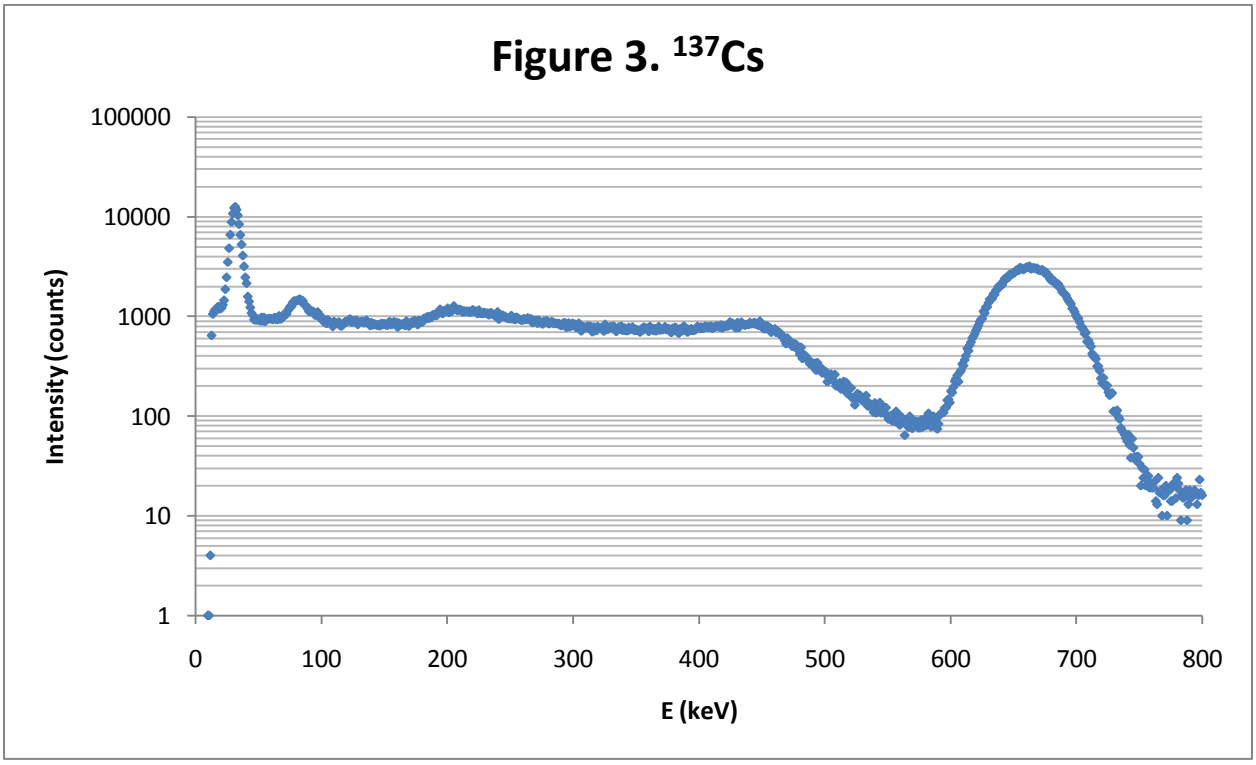

4.1.2d ^{57}Co

There was only one photopeak found for ^{57}Co, as seen in Figure 4. This is likely due to the two expected photopeaks being too close to separately identify with the equipment used. The peak, at 130 keV, has an associated Compton edge at 45 keV and backscatter peak at 80 keV. The photopeak and Compton edge fall in between the two expected values corresponding to the two expected peaks; however, the backscatter peak is 3.1% below the energy of the expected peaks and 9.9% below the higher. The photopeak is 6.6% above the energy of the lower expected peak and 4.4% below the energy of the higher expected peak. The Compton edge is 14% above the lower expected value and 4.7% below the higher expected value.

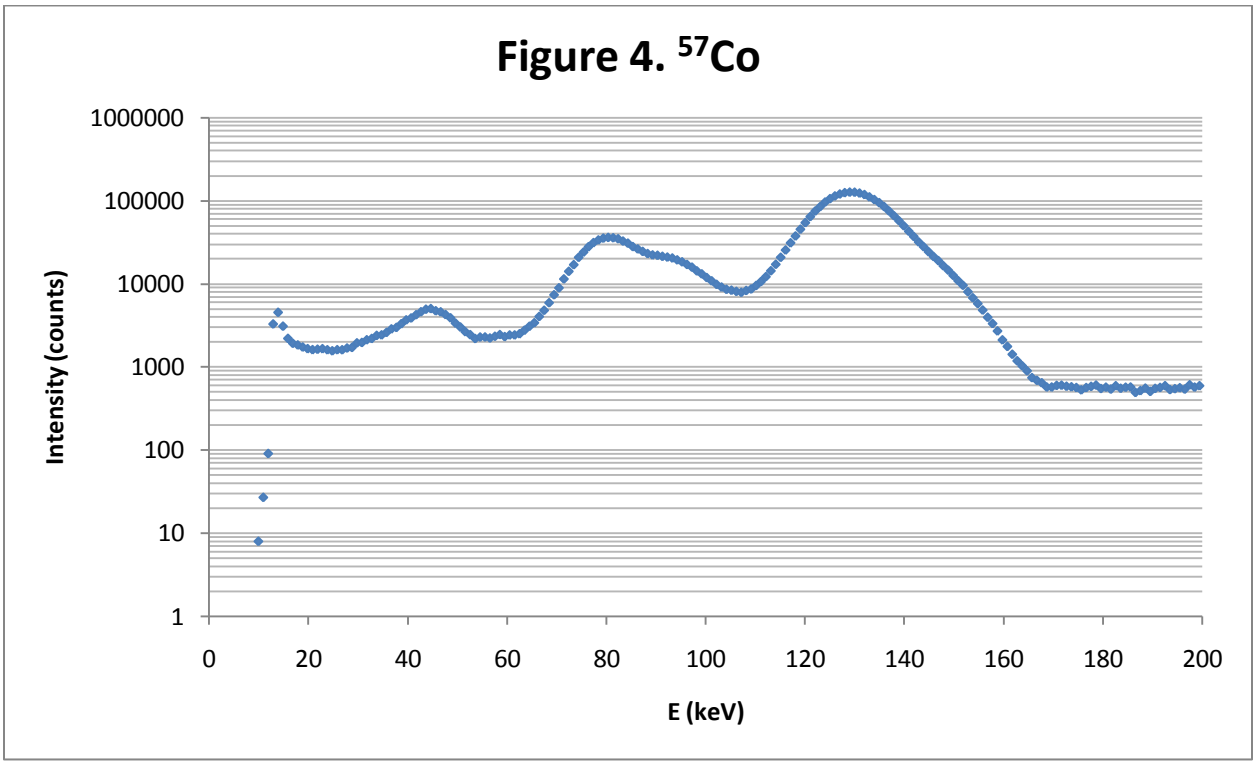

4.1.2e ^{60}Co

There were two photopeaks found for ^{60}Co, as seen in Figure 5. The first, at 1173 keV, has an associated Compton edge at 932 keV. The experimental peak matched the expected peak. The experimental Compon edge, however, was 3.2% below the expected value. The second, at 1315 keV, has an associated Compton edge at 1059 keV. These values deviate from the expected values by 1.4% and 5.3%, respectively. The backscattering peaks were too close to separately identify, and 214 keV was found for both. This deviates from the expected value associated with the 1173 keV photopeak by 2.0% and the value associated with the 1315 photopeak by 0.2%.

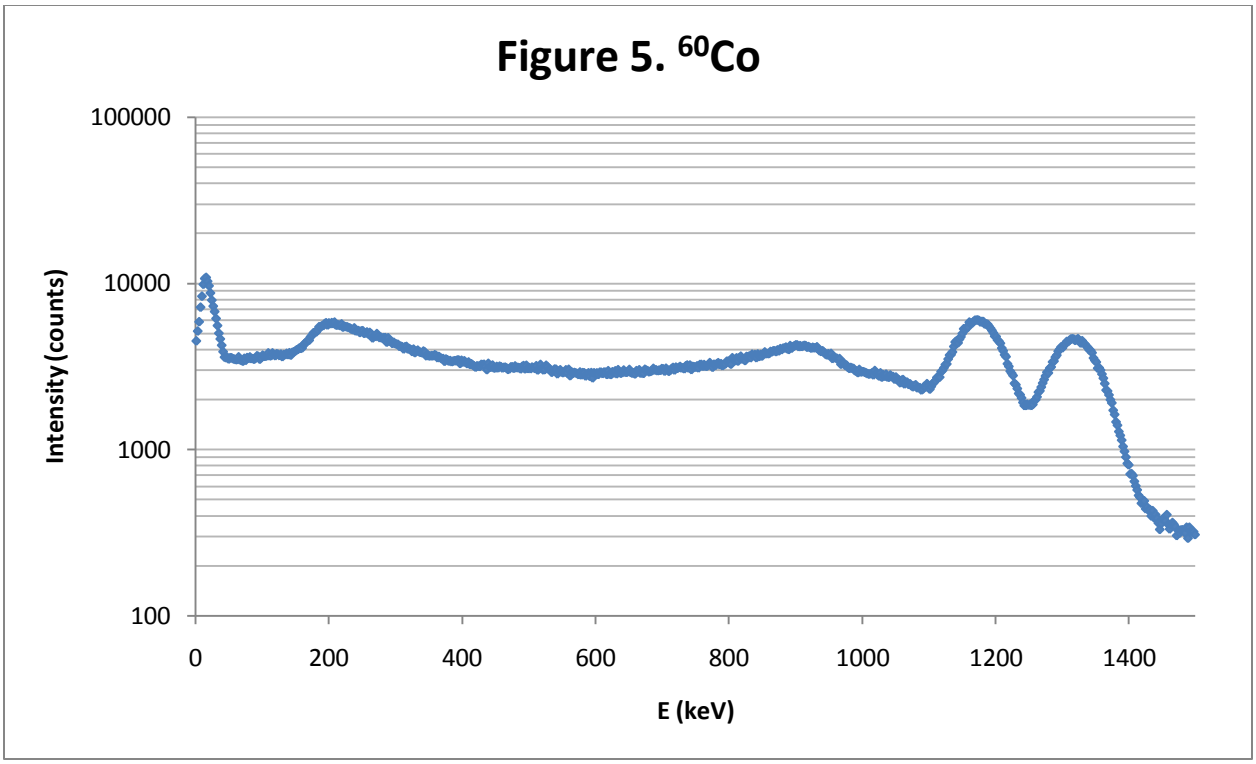

4.1.2f ^{54}Mn

There was one photopeak found for ^{54}Mn, as seen in Figure 6. The peak, at 818 keV, has an associated Compton edge at 589 keV and backscatter peak at 237 keV. These values deviate from the expected values by 2.0%, 7.9%, and 21.1%, respectively.

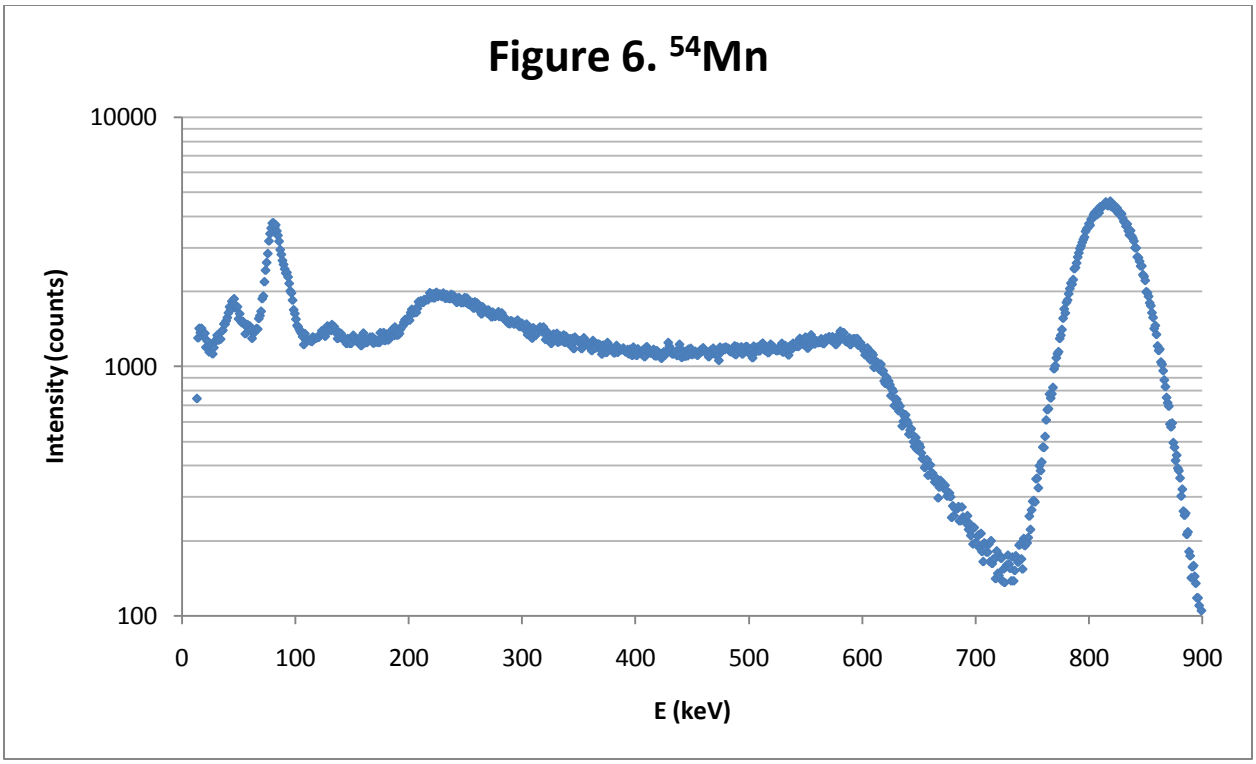

4.1.2g 22Na

There were two photopeaks found for ^{22}Na, as seen in Figure 7. The first, at 513 keV, has an associated Compton edge at 312 keV and backscatter peak at 153 keV. These values deviate from the expected values by 0.4%, 8.4%, and 10.2%, respectively. The second, at 1277 keV, has an associated Compton edge at 1044 keV and backscatter peak at 210 keV. These values deviate from the expected values by 0.2%, 1.7%, and 1.3%, respectively.

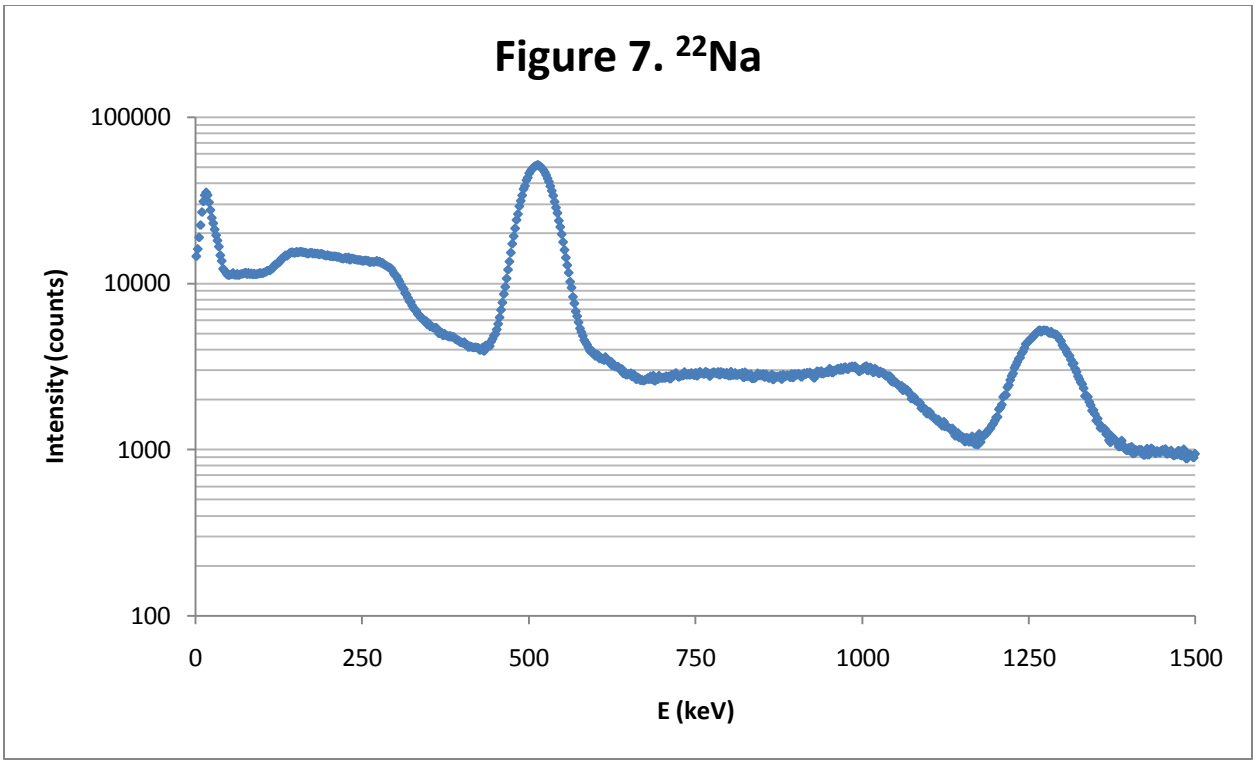

4.1.2h 207Bi

There were three large photopeaks found for ^{207}Bi, as seen in Figures 8 and 9. The first, at 568 keV, has an associated Compton edge at 384 keV and backscatter peak at 189 keV. These values deviate from the expected values by 0.3%, 2.4%, and 7.1%, respectively. The next, at 1073 keV, has an associated Compton edge at 805 keV and backscatter peak at 228 keV. These values deviate from the expected values by 0.9%, 6.1%, and 10.7%, respectively. The last, at 1598 keV, has an associated Compton edge at 1387 and backscatter peak at 255 keV. These values deviate from the expected values by 9.7%, 10.3%, and 14.2%, respectively. Another peak was expected, at around 894 keV. This peak was unidentifiable, as it lies between the two areas in which the equipment was calibrated to accurately measure.

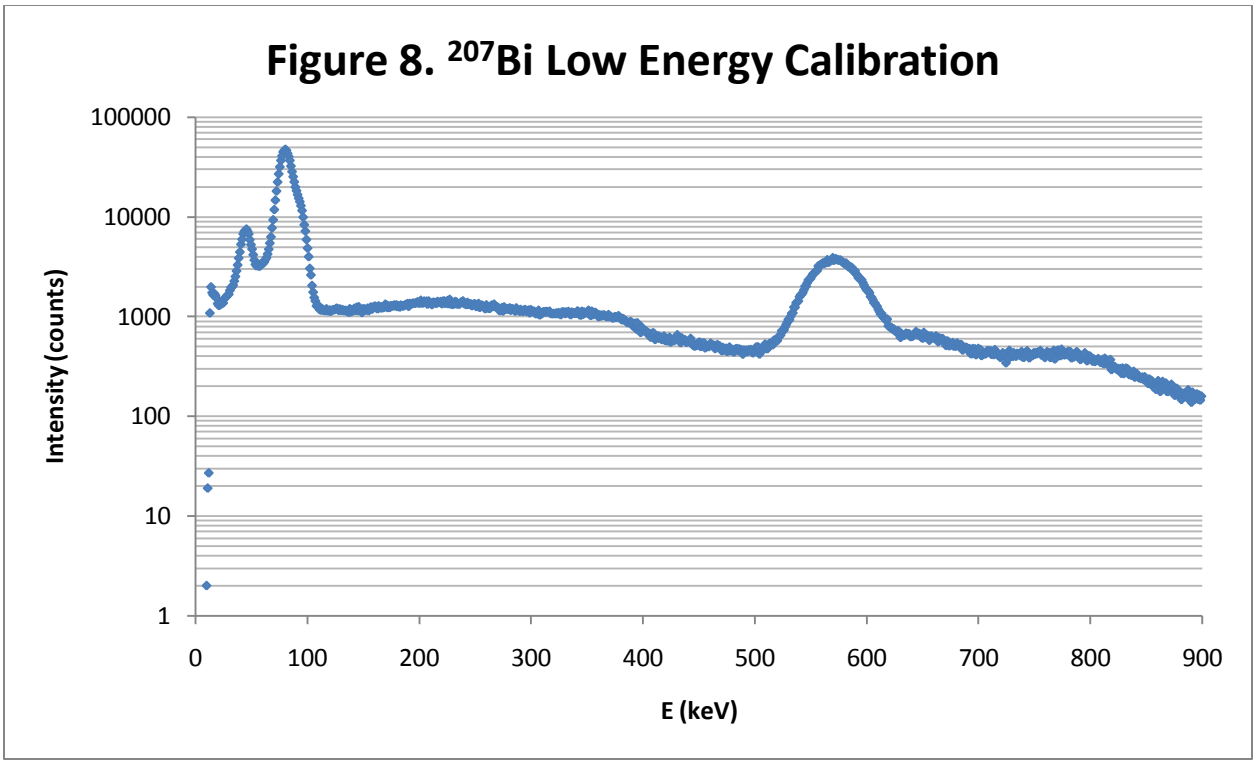

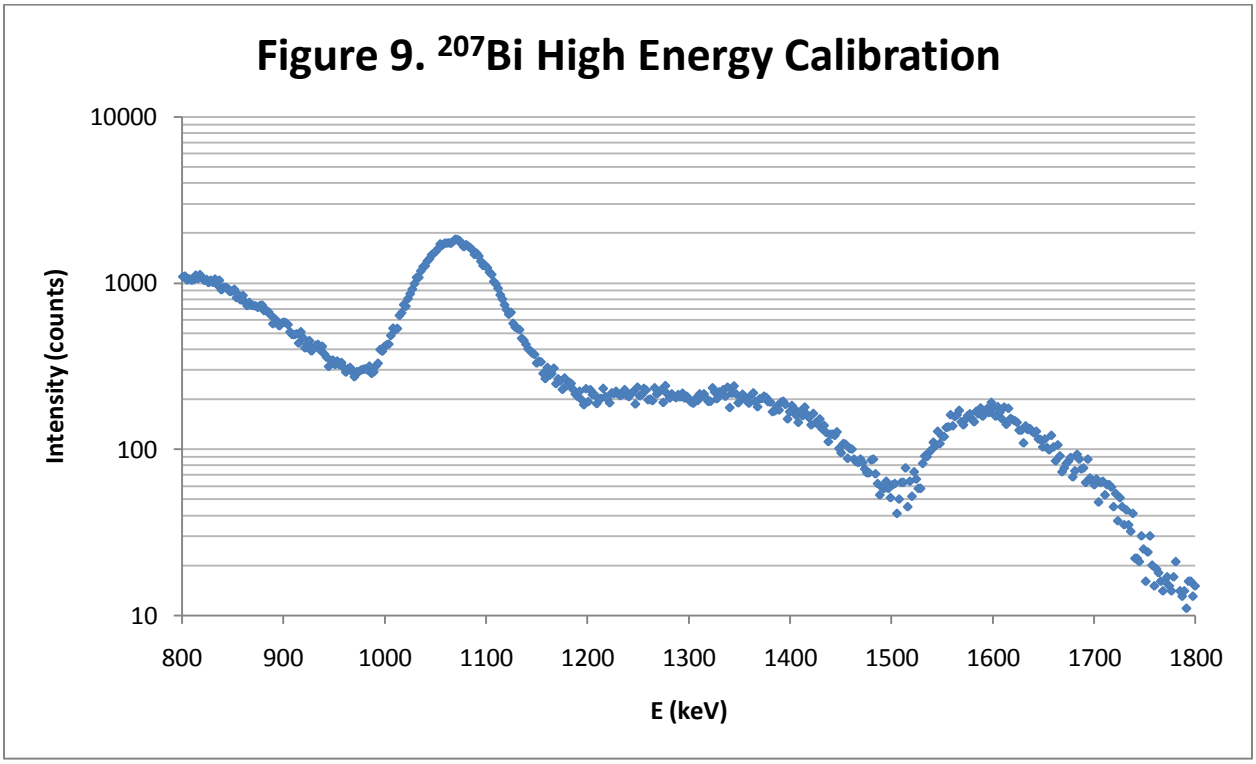

4.2 Determination of an Unknown Source

Using the previous verification as proof that the theory is correct, the spectrum of an unknown source was analyzed in order to determine its composition. It was known that this source

was comprised of both ^{65}Zn and ^{137}Cs and by examining the spectrum output of the software, it was possible to approximate the ratios of these elements in the source. By comparing the relative intensities of the known ^{137}Cs 662 keV photopeak and backscatter peaks, which should contain contribution from both measured peaks to that same ratio in the pure ^{137}Cs sample, a composition of ~1/3 ^{137}Cs and ~2/3 ^{65}Zn was calculated.

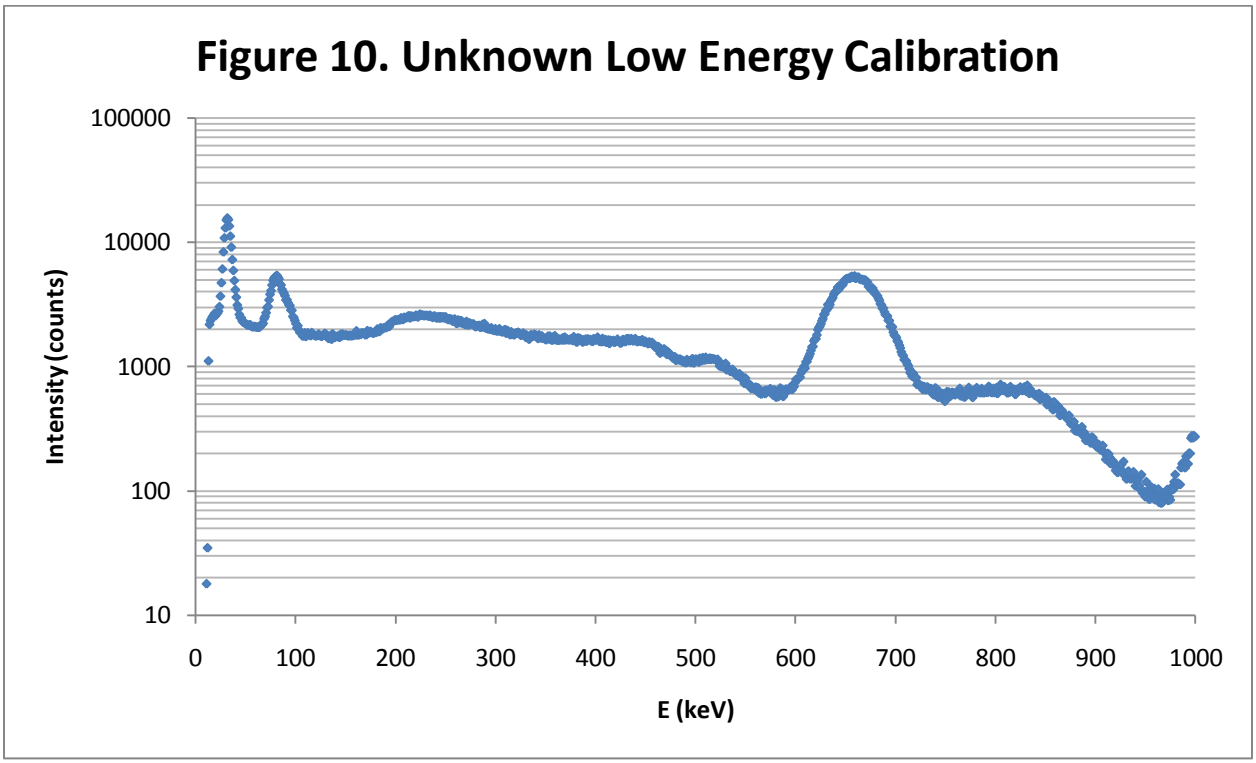

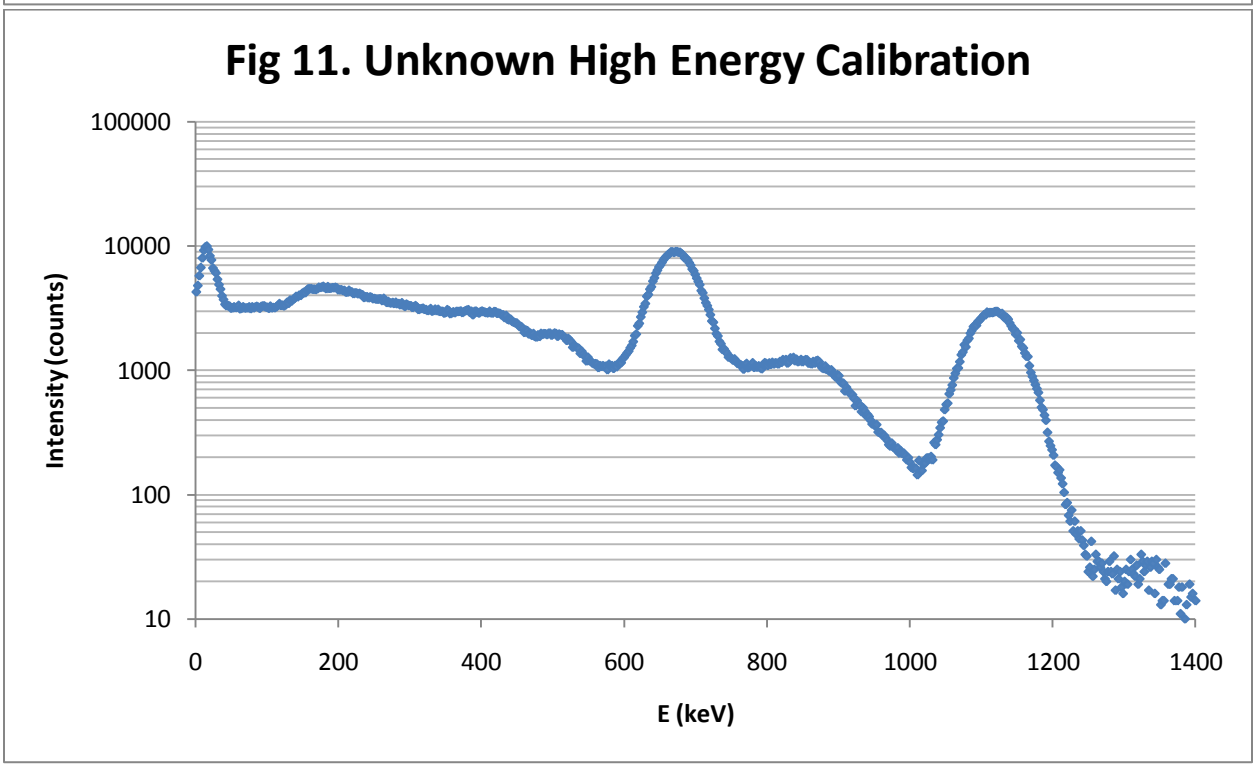

4.3 Determination of the Electron Rest Mass

Finally in the analysis, the data obtained through scintillation counting was used to experimentally determine the electron rest mass. This was done by solving the equation given for the Compton edge (2.3) for the rest mass of the electron (mc^2). Using the Compton edge determined from the each of the gamma ray spectra, this equation was then solved, giving an experimentally-determined value of the rest mass of 573 keV with a standard deviation of 95.8 keV.

4.4 Density Normalized Mass Attenuation Coefficient

4.4.1 Low Energy Coefficient

For the low energy density normalized mass attenuation coefficient determination, the 122 keV and 136 keV photopeaks of ^{57}Co were measured through varied amounts of Lead and Copper shielding.

4.4.1a Lead

The low energy coefficient for Lead was determined to be 2.760. One 0.369 mm sheet of Lead was required to attenuate the 122 keV peak by 73% and the 136 keV peak by 65%.

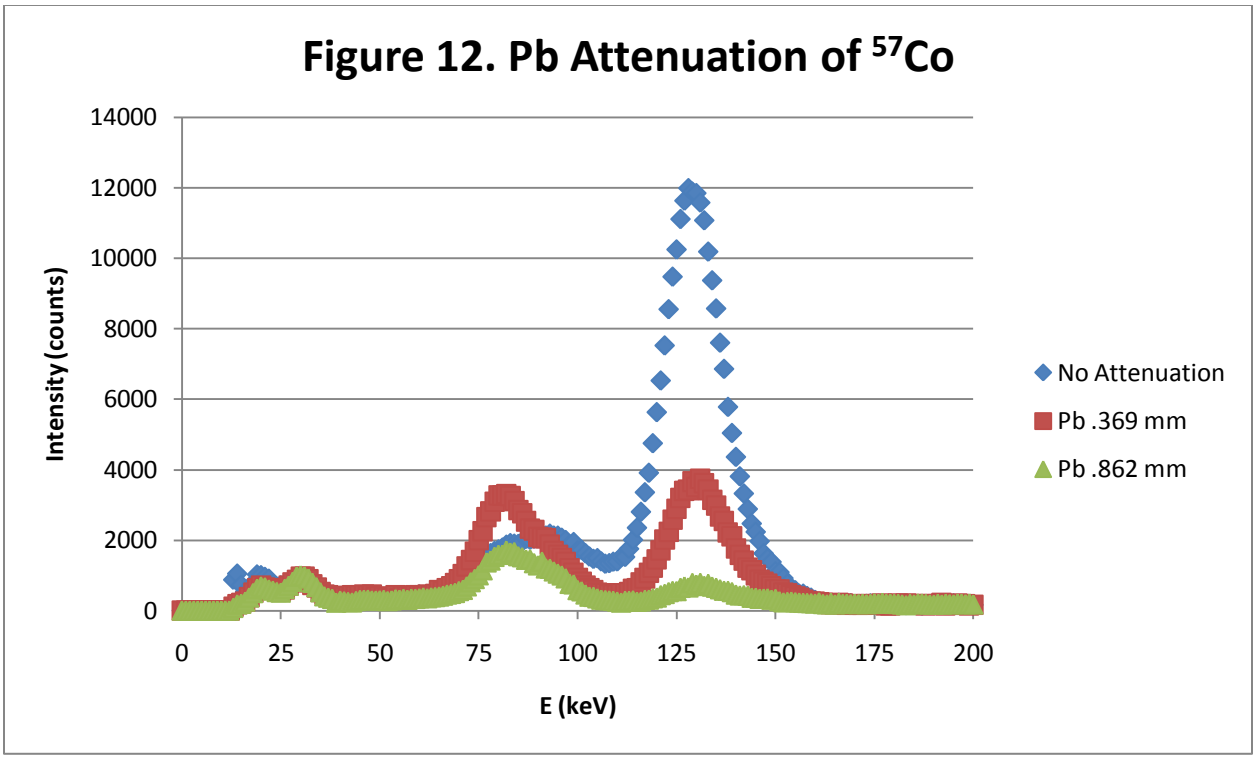

4.4.1b Copper

The low energy coefficient for Copper was determined to be 0.224. 6.31 mm of Copper shielding was required to attenuate the 122 keV peak by 70% and the 136 keV peak by 75%.

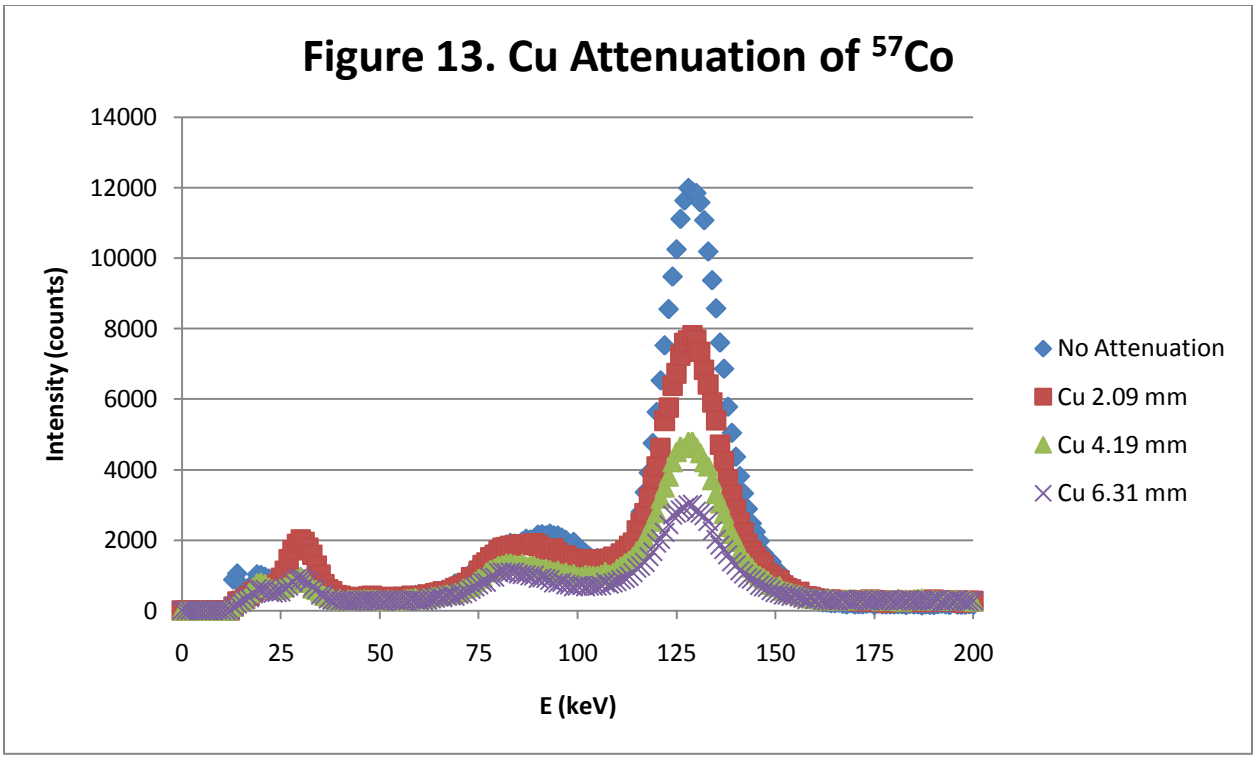

4.4.2 High Energy Coefficient

4.4.2a Lead

The high energy coefficient for Lead was determined to be 157.01. 11.83 mm of Lead shielding was required to attenuate the 1173 keV peak by 48% and the 1333 keV by 43%.

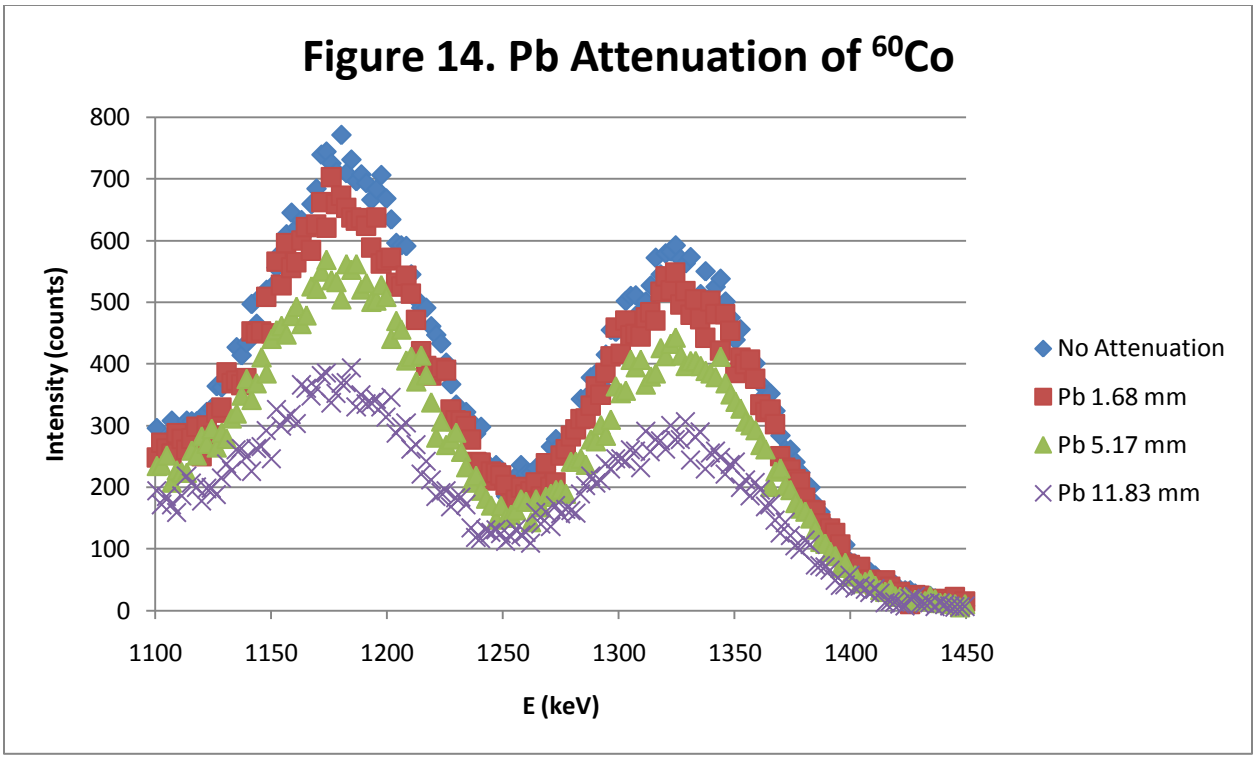

4.4.2b Copper

The high energy coefficient for Copper was determined to be 45.207. 37.24 mm of Copper shielding was required to attenuate the 1173 keV peak by 71% and the 1333 keV by 67%.

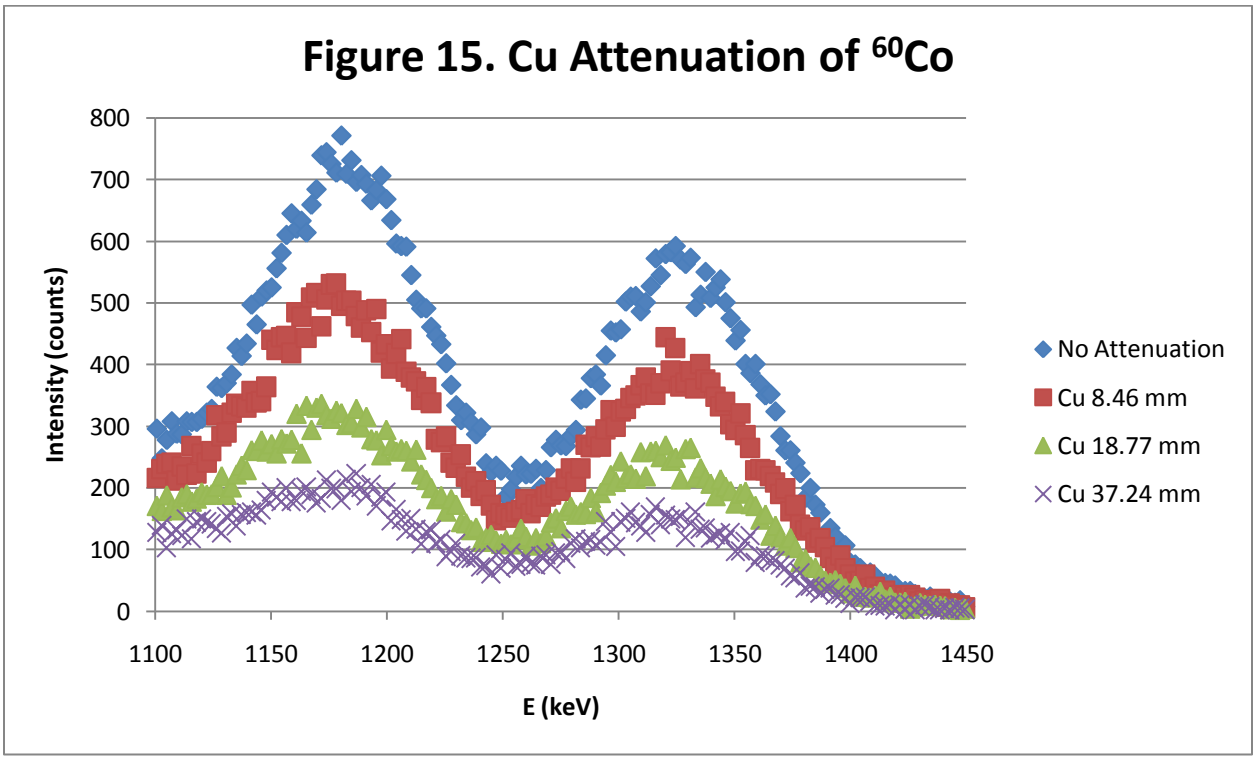

5 Conclusion

In this experiment, scintillation was used to analyze the spectra of various radioactive sources. In doing so, students have become much more familiar with several aspects of gamma rays. The photoelectric effect, Compton and Rayleigh scattering, and pair production were observed, with photopeaks, Compton edges, and backscatter peaks being identified for eight different known sources. This allowed students to experimentally verify existing decay theories and determine the composition ratio of an unknown source to be approximately one-third ^{137}Cs and two-thirds ^{65}Zn. From the gathered data, the rest mass of the electron was experimentally determined to be 573 keV. Lastly, the density normalized mass attenuation coefficient of lead and copper at both a low and high gamma ray energy range was calculated from experimental data.

6 Appendix

Element	Peak (keV)	Compton Edge (keV)	Backscatter (keV)
^{133}Ba	81	19.49777117	61.50222883
	276	143.3226717	132.6773283
	303	164.3849597	138.6150403
	356	207.2542927	148.7457073
	384	230.5801407	153.4198593
^{109}Cd	88	22.54439592	65.45560408
^{137}Cs	662	477.6501362	184.3498638
^{57}Co	122	39.42781457	82.57218543
	136	47.24393359	88.75606641
^{60}Co	1173	963.1984599	209.8015401
	1333	1118.59553	214.4044696
^{54}Mn	835	639.3626777	195.6373223
^{22}Na	511	340.6666667	170.3333333
	1275	1062.152891	212.8471088
^{207}Bi	569.7	393.308398	176.391602
	894	695.2901261	198.7098739
	1063.66	857.6462261	206.0137739
	1770.2	1546.926021	223.2739794

Table 1: Theoretical Compton edges and backscatter peaks for the full absorption peaks of the sources

Element	Peak (keV)	Compton Edge (keV)	Backscatter (keV)	mc^2 (keV)
^{133}Ba	87	30	68	330.6
	310	169	124	517.2781065
	370	207	154	582.705314
^{109}Cd	93	21	76	637.7142857
^{137}Cs	663	454	205	610.4273128
^{57}Co	130	45	80	491.1111111
^{60}Co	1173	932	214	606.6373391
	1315	1059	214	635.769594
^{54}Mn	818	589	237	636.0679117
^{22}Na	513	312	153	660.9807692
	1277	1044	210	570.0019157
^{207}Bi	568	384	189	544.3333333
	1073	805	228	714.4447205
	1598	1387	255	486.1975487

Table 2: Experimental Compton edges, backscatter peaks, and electron rest masses for the full absorption peaks of the sources

7 References

Nuclear Decay Reference:
Tipler, Paul, Ralph Llewellyn. Modern Physics 5ed. New York: W.H. Freeman and Company, 2008.

Laboratory Manual:
LeClair, Patrick. "PH255: Modern Physics Laboratory". University of Alabama, 2010.